Yields of In and Sn products from thermal- and 14-MeV-neutron-induced fission of ^{235}U

Tomasz M. Semkow, Arthur C. Wahl, and Larry Robinson
Department of Chemistry, Washington University, St. Louis, Missouri 63130
(Received 11 June 1984)

The fractions of tin fission products formed independently and by decay of indium isotopes were determined for $A=121$, 123, 125, 127, and 128 from thermal-neutron-induced fission of ^{235}U, and for $A=121$, 123, 127, and 128 from 14-MeV-neutron-induced fission of ^{235}U. The procedure involved on-line chemical separation of indium and tin fission products by use of a continuous-extraction method during irradiation and beta-activity measurements of purified tin samples after decay of indium precursors. Measured fractions of tin isotopes formed directly or by beta decay combined with their cumulative yields and mass-number (chain) yields allowed calculation of independent and/or cumulative yields for the nuclides studied. The yields of indium isotopes agree with complementary technetium yields measured radiochemically, but they are lower than most indium yields measured mass spectrometrically and most complementary technetium yields measured with recoil separators. The yield data were used to determine mass- and charge-distribution parameters $\sigma_{A'}$, $\Delta A'$, $Y(Z)$, σ_Z, and ΔZ for thermal-neutron-induced fission of ^{235}U. The values of $\sigma_{A'}$ and σ_Z are similar to the averages of values derived for other elements and mass numbers. $\Delta A'$ has a pronounced peak at $Z=50$, and the elemental yield decreases sharply from $Y(Z=50)=4.0\%$ to $Y(Z=49)=0.1\%$. The ΔZ function increases abruptly near $Z=50$, changing from ~ -0.45 to positive values, as indicated by earlier experimental data, but inconsistent with the scission-point theoretical predictions. These effects, associated with the fifty-proton shell, diminish at higher excitation energy.

INTRODUCTION

The research described in this paper was undertaken to measure fission yields of indium and tin isotopes in the mass-number range $A=121-128$ for thermal-neutron-induced fission of ^{235}U, and for 14-MeV-neutron-induced fission of ^{235}U. The independent yields of Sn isotopes are predicted to be enhanced, while those of In isotopes are predicted to be lowered, relative to those derived from extrapolation of average mass- and charge-distribution systematics, due to a closure of the fifty-proton shell.[1,2] The use of two neutron energies, thermal and 14 MeV, should give information about the effect of excitation energy on the influence of the fifty-proton shell on fission yields.

It has been recognized for a long time that closed nucleon shells affect yields of fission products. For example, it was observed that the light side of the heavy peak of mass-yield curves coincided for many fission processes, e.g., thermal-neutron-induced fission of ^{233}U, ^{235}U, ^{239}Pu, and spontaneous fission of ^{252}Cf.[3] This was attributed to the formation of heavy fragments close to the $Z=50$ and $N=82$ nucleon shells. Also, the transition from the double-peaked mass distribution for fission of $^{254,256,257}Fm$ to single-peaked distributions for $^{258,259}Fm$ was explained by favored formation of fragments with masses and charges close to the $N=82$ and $Z=50$ shells.[4] ^{259}Md shows a broad symmetric mass distribution,[5] possibly with a small dip at the top, which can be interpreted as the occurrence of considerable asymmetric fission.[2]

Various theoretical approaches were able to show semiquantitative agreement with experimental yields by including shell corrections, which modulate the potential energy of a deformed liquid drop. For example, Wilkins *et al.*[6] explained in their scission-point model the transition from single-peaked fission of Po isotopes through triple-peaked fission of Ra isotopes to double peaked fission of most actinide nuclides using distorted neutron shells.

Some information about yields of indium isotopes in the mass-number range $A=121-128$ for thermal-neutron-induced fission of ^{235}U was obtained earlier by Erdal *et al.*[7] from measurement of formation modes of tin isotopes. The method involved radiochemical batch separation of indium and tin fission products. Also, mass-spectrometrically measured $^{124-132}In$ yields for thermal-neutron-induced fission of ^{235}U have also been published recently.[8] Yields of Tc isotopes, which are complementary to In, are of interest too. (Complementarity is defined as $Z_L+Z_H=92=Z$ of uranium.) Technetium yields were measured radiochemically[9,10] and also by use of the Hiawatha[11] and Lohengrin[12] recoil separators.

Our experiments involved continuous radiochemical separation of newly formed indium and tin fission products from irradiation of ^{235}U with neutrons. Solvent extraction was used for separation, which was performed continuously with a SISAK system. (SISAK is an abbreviation for the short-lived isotopes studied by the Akufve method, Akufve being the Swedish abbreviation for "apparatus for continuous measurement of distribution factors in solvent extraction;" see Ref. 13, and references therein.) After irradiation and complete decay of indium to tin fission products, the latter were separated and purified radiochemically, and beta decay of the resulting tin samples was followed.

The method is a relative one. Indium nuclides were not directly measured during or after irradiation. Instead, tin descendants were measured, which allowed determination of fractions of tin nuclides which were formed in fission via particular paths, i.e., independently or by beta decay. A similar tin-formation-mode method has been used before.[7] Cumulative-independent yields of indium products and independent yields of tin products can be calculated from tin formation fractions and known cumulative fission yields of tin and mass-number (chain) yields.

The experimental section reveals some details of irradiation-separation procedures and beta-decay measurements. The data-reduction section describes resolution of beta-decay data and calculation of fission yields. The discussion section deals with comparison of various types of yield measurements and with nuclear charge- and mass-distribution parameters in the vicinity of the $Z=50$ shell. Finally, in the Appendix, equations of radioactive decay and growth are presented, which include the continuous irradiation-separation concept and a matrix notation.

EXPERIMENTAL

The actual fission experiments were preceded by a study of solvent-extraction chemistry of tracer amounts of Sn, In, and neighboring elements, Ag, Cd, Sb, as well as U.[1,14] Both batch extraction and continuous extraction with a SISAK system were investigated. In the SISAK system two phases, aqueous and organic, are mixed during flow through a static mixer. Then the mixed phases are separated by the centrifugal force of up to 30000g in an H-10 centrifuge. The results of extraction experiments with the SISAK system are shown in Table I.

Figure 1 shows a diagram of the setup for the on-line irradiation-separation experiments. The aqueous phase (see Table I) had a volume of 2.0 l and contained about 10 g of uranium (enriched to 93.2% in ^{235}U) as $UO_2(NO_3)_2$. The aqueous phase was circulated with a mean time of $u=212.6$ sec. Solution flowed through a tank target.[15] The target was subjected either to a thermal-neutron flux of $\sim 3\times 10^8$ cm^{-2}sec^{-1} from the Washington University cyclotron or to the average $\sim$14-MeV-neutron flux of $\sim 3\times 10^8$ cm^{-2}sec^{-1} from a neutron generator. The mean holdup time, T, of the solution in the target was about 2 sec. Injection of I_2 ensured oxidation of Sn(II) to Sn(IV).

The main variable in this experiment was the delay time (symbol τ) required for passage of the aqueous phase from the target outlet to about the middle of the separation assembly. The delay time was varied for different experiments from 0.7 to $\sim$20 sec by changing the length and diameter of a connecting pipe. The chemical separation was assumed to occur halfway between the start of mixing of phases and their separation in the centrifuge. Phase separation was believed to be essentially complete midway through the centrifuge. The total time during which separation could have occurred was 0.8 sec, and the midpoint of this period was chosen as the separation time with an uncertainty of ± 0.4 sec, which is then the uncertainty in τ.

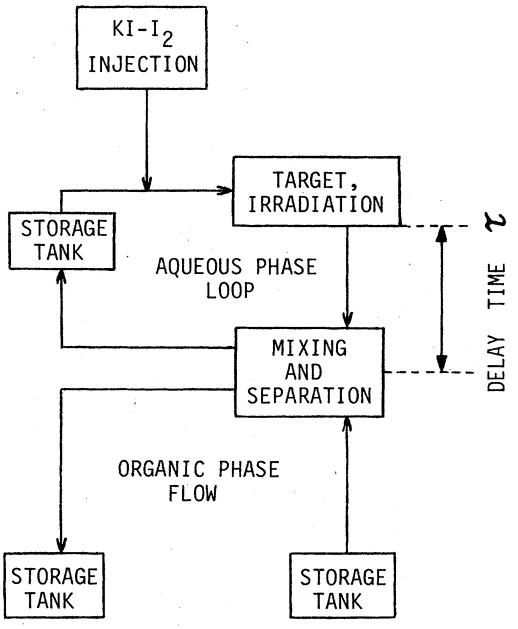

FIG. 1. Diagram of setup for irradiation experiments described in the text.

The organic phase (see Table I) flowed from one storage tank to another through the mixer and centrifuge. About 20 l of organic phase were used in each experiment. The flow rate for both aqueous and organic phases was 9.5 ± 0.2 ml/sec. The total irradiation time was about 30 min.

This setup allowed separation of more than one-half of the following indium fission products, present at the time of separation, into the organic phase: 3.88-min ^{121}In^m and 23.1-sec ^{121}In (Ref. 16), 47.8-sec ^{123}In^m and 5.98-sec ^{123}In (Ref. 17), 12.2-sec ^{125}In^m and 2.33-sec ^{125}In (Ref. 17), 3.7-sec ^{127}In^m (Ref. 17), 1.12-sec ^{127}In (average from Refs.

TABLE I. Single-step extraction fractions, c, of tracer quantities of various elements separated from aqueous solution[a] to organic solvent[b] using the continuous SISAK method.

Ag(I)	Cd(II)	In(III)	Sn(II)	Sn(IV)	U(VI)
0.986	0.984	0.528 ± 0.042	0.021 7.9×10^{-4}[c]	8.5×10^{-4}	6.2×10^{-4}

[a] 0.1N KI, 0.1N H_2SO_4, 0.021M $UO_2(NO_3)_2$ solution.
[b] 85 vol % methyl isobutyl ketone and 15 vol % cyclohexanone.
[c] With injection of I_2 solution to oxidize Sn(II) to Sn(IV).

17–20), and 0.90-sec ^{128}In (average from Refs. 8, 17, 19, 21, and 22), the references given being the sources of the half-life values. Also, most of the Ag and Cd precursors were extracted into the organic phase, while most of the Sn fission products remained in the aqueous phase. The small fractions of Sn extracted, F, depend slightly on the half-life of the Sn nuclide and are higher than single-step extraction fractions, c, from Table I due to recirculation of the aqueous phase. They were determined in a separate experiment.[1] For example, $F=2.385\times10^{-3}$ for 9.64-d ^{125}Sn.

The pipes and storage tank for the water phase were shielded from scattered neutrons with a Cd sheet. Still some activity was generated outside the target. The fractions, f, of activity formed in the target were determined in separate experiments[1] and resulted in $f=0.928$ for thermal-neutron and $f=0.996$ for 14-MeV-neutron irradiations.

After an irradiation, the indium isotopes were allowed to decay to tin, and tin was separated and purified from both the organic and aqueous phases using radiochemical procedures.[1,23] Tin samples were then mounted for beta-activity measurements, and their decay was followed with beta-proportional counters.[1] The time scale of these experiments allowed measurement of the following tin nuclides: 27.0-h ^{121}Sn, 40.1-min ^{123}Sn^m, 129.3-d ^{123}Sn, 9.64-d ^{125}Sn, 2.10-h ^{127}Sn, and 59.3-min ^{128}Sn. After about 30 h of measurement the nuclides with 40.1-min, 2.10 h, and 59.3-min periods had decayed completely, and considerable amounts of antimony and tellurium daughter products had grown in. Therefore, tin samples were repurified, and remounted for measurement, which continued for several weeks.[1]

DATA REDUCTION

Decay data for tin isotopes and antimony and tellurium descendants were resolved into exponential components using a modified least-squares program, CLSQ.[24] Counting data were corrected for radiochemical yield, dead-time losses, and decay during a counting interval by the program. The program calculated counting-rate intercepts, I_i, at a chosen time (e.g., end of irradiation or separation time) for each of several components with decay constants λ_i.

Intercepts I_i are functions of numbers of radioactive atoms, decay constants, and counting efficiencies. Frequently calculations included subtraction of known components, e.g., intercepts calculated from those determined for repurified samples were subtracted from measured activities of original samples before least-squares reduction of the data. Also, the intercept ratios of genetically related nuclides, determined in separate experiments, were used to facilitate the resolutions. (See Ref. 1 for a complete description of decay-data analysis.)

For each tin component, intercepts from organic- and water-phase samples, I^{org} and I^{wat}, respectively, were corrected for counting efficiencies and converted to the same time, then the total intercept activity was calculated, $I^{tot}=I^{org}+I^{wat}$. The intercept ratios I^{org}/I^{tot}, the fraction of activity found in the organic phase, were then plotted versus delay time τ for each tin nuclide. Figures 2–4 show plots for ^{123}Sn^m, ^{125}Sn, and ^{128}Sn. The solid curves represent functions that best represent the points and are described below. The slopes of the curves are related to the half-lives of the indium precursors, i.e., 5.98-sec ^{123}In and 47.8-sec ^{123}In^m, 2.33-sec ^{125}In, and 0.90-sec ^{128}In for Figs. 2–4, respectively. The dashed lines in Figs. 3 and 4 correspond to the fractions, F, of Sn extracted. If there were no In precursors extracted, the solid curves would be flat, indicating the extraction of Sn only. The vertical components of the error bars in Figs. 2–4 include errors from least-squares resolution of counting data into components by the CLSQ program and errors due to efficiency corrections. The horizontal components represent uncertainties in delay time τ of ±0.4 sec.

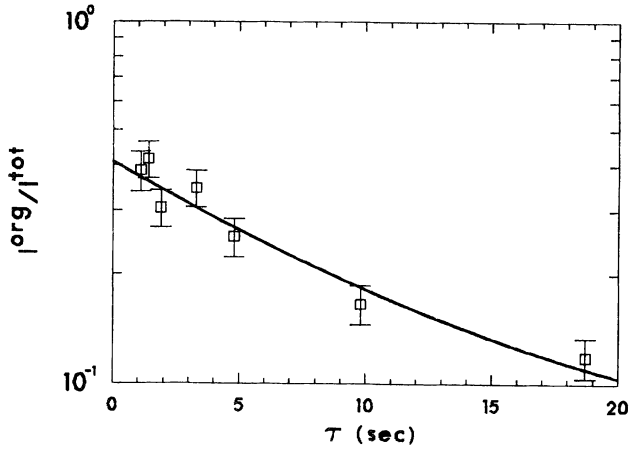

FIG. 2. Intercept ratio I^{org}/I^{tot} vs delay time τ for ^{123}Sn^m from thermal-neutron-induced fission of ^{235}U. The solid curve represents the best fit to the data.

The functions fitted to intercept ratios are based on radioactivity decay and growth equations. Standard radioactive decay-growth equations were not applicable be-

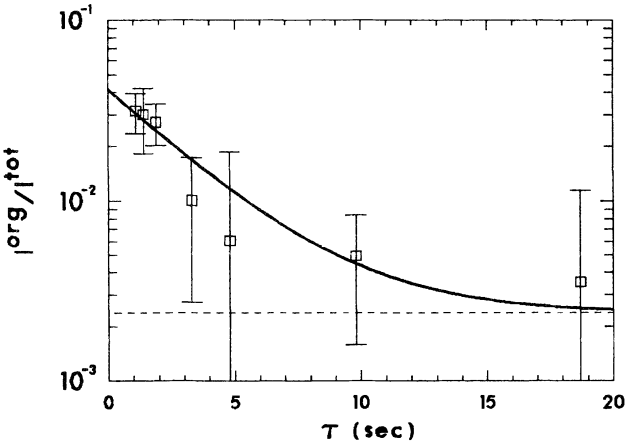

FIG. 3. Intercept ratio I^{org}/I^{tot} vs delay time τ for ^{125}Sn from thermal-neutron-induced fission of ^{235}U. The solid curve represents the best fit to the data. The dashed line represents the fraction of Sn nuclides extracted into the organic phase.

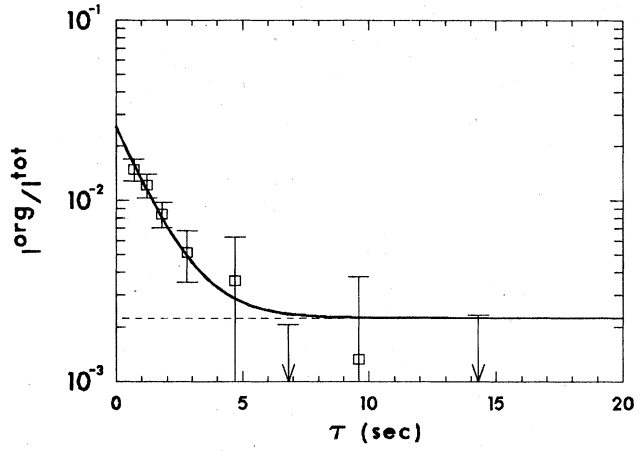

FIG. 4. Intercept ratio I^{org}/I^{tot} vs delay time τ for ^{128}Sn from 14-MeV-neutron-induced fission of ^{235}U. The solid curve represents the best fit to the data. The dashed line represents the fraction of Sn nuclides extracted into the organic phase.

cause of the flow of solutions and because of the complicated decay and extraction patterns. Using a tank-target model, we derived the radioactive decay-growth equations for species moving in a steady-state flow. Due to circulation of the irradiated solution, we developed two models describing the repetitive extraction of species: a fractional model useful for large extraction and short half-life and a differential model useful for small extraction and rather long half-life. All the equations were expressed in a matrix notation, which simplifies the problems usually associated with many-membered chains with branching decay. The equations are given in the Appendix and include explicit expressions for the P and P^{-1} decay-growth matrices, which we derived.

The equations were programmed as subroutines to a modified general least-squares program, ORGLS.[25] Fractional independent (cumulative) yields, half-lives, and branching ratios could be determined. For example, proper behavior of the programs was checked by determination of the half-lives for short-lived ^{127}In and ^{128}In. The values found, $T_{1/2}(^{127}\text{In})=1.16\pm0.17$ sec and $T_{1/2}(^{128}\text{In})=1.04\pm0.09$ sec, agree with average values from physical measurements of 1.12 ± 0.03 and 0.90 ± 0.08 sec, respectively. For the yield determinations, however, literature values were used for half-lives (given earlier) and for branching ratios.[1]

The fractional independent (FI) or cumulative (FC) yields, FI_i or FC_i, for members of a particular decay chain were determined by specifying the fractional cumulative yield, FC_n, of the tin nuclide measured. However, by putting arbitrarily $\text{FC}_n=1$ the parameters determined are the fractions of the tin nuclide formed via particular paths.

The formation modes of tin nuclides are given in Table II. For ^{121}Sn, ^{123}Sn^m, ^{125}Sn, ^{127}Sn, and ^{128}Sn, which were measured, fractions formed are those derived from the least-squares analysis. For other nuclides, ^{121}Sn^m, ^{123}Sn, ^{125}Sn^m, and ^{127}Sn^m, which were not measured, fractions formed were calculated, as described in Ref. 1, using measured fractions from this investigation, as well as from Ref. 7, literature values of branching fractions, and cumulative yields of tin nuclides and/or mass-number (chain) yields from Rider's compilation.[26]

Use of formation-mode values and literature values for antimony fission yields allowed calculation of independent (cumulative) yields of a number of indium and tin nuclides and of ^{121}Ag and ^{121}Cd. The results are shown in Table III; Table IV contains the fractional yields. The formation modes for 14-MeV-neutron-induced fission are less useful than for thermal-neutron-induced fission, because there is little experimental information about cumulative yields of tin nuclides from 14-MeV-neutron-induced fission, so yield calculations are not possible.

Some features of the calculations are described below. For $A=121$ there are six components: 0.72-sec ^{121}Ag, 8.3-sec ^{121}Cd^m, 12.5-sec ^{121}Cd, 3.88-min ^{121}In^m, 23.1-sec ^{121}In, and 27.0-h ^{121}Sn, and there are insufficient data for calculation of all six yields. The data could be well represented by assuming the fractions of ^{121}Cd, ^{121}In^m, and ^{121}Sn formed directly to be $0.0^{+0.05}_{-0.00}$; then the yields for the other three nuclides could be determined and are

TABLE II. Formation modes of Sn nuclides for neutron-induced fission of ^{235}U.

Nuclide	Neutron energy	Fraction of Sn formed by β^- decay of In^m	Fraction of Sn formed by β^- decay of In^g	Fraction of Sn formed independently
^{121}Sn^m	thermal		0.77±0.26	0.23±0.43
^{121}Sn	thermal	0.14±0.15	0.86±0.29	$0^{+0.05}_{-0.00}$
^{121}Sn	14 MeV	0.25±0.12	0.75±0.23	$0^{+0.05}_{-0.00}$
^{123}Sn^m	thermal	0.185±0.046	0.797±0.115	0.018±0.069
^{123}Sn^m	14 MeV	0.185±0.077	0.755±0.193	0.060±0.117
^{123}Sn	thermal		0.195±0.033	0.805±0.076
^{125}Sn^m	thermal	<0.43	0.684±0.115	<0.43
^{125}Sn	thermal		0.129±0.019	0.871±0.019
^{127}Sn^m	thermal		0.375±0.100	$^{<0.753}_{>0.262}$
^{127}Sn	thermal		0.052±0.013	0.948±0.013
^{127}Sn	14 MeV		0.068±0.017	0.932±0.017
^{128}Sn	thermal		0.044±0.022	0.956±0.022
^{128}Sn	14 MeV		0.133±0.042	0.867±0.042

TABLE III. Fission yields (%) for thermal-neutron-induced fission of ^{235}U. The first yield is cumulative, the rest are independent for a particular A. Both isomers are included, where appropriate.

A	Ag	Cd	In	Sn
121	0.0027±0.0027	0.0075±0.0035	0.0023±0.0013	0.0004±0.0007
123			0.0140±0.0020	0.0018±0.0010
125			$0.0162^{+0.0052}_{-0.0034}$	$0.0128^{+0.0049}_{-0.0028}$
127			0.0283±0.0086	0.0887±0.0126
128			0.0147±0.0074	0.320 ±0.013

shown in Table III.

The yield values for 5.98-sec ^{123}In and 47.8-sec ^{123}In^m reported in Tables II–IV and corresponding to the curve in Fig. 2 were determined without consideration of ^{123}Ag and ^{123}Cd precursors. The half-life of 0.39 sec (Ref. 22) for ^{123}Ag is too short to have been detected or to have affected our results appreciably. However, a ~2-sec half-life[27,28] for ^{123}Cd is inconsistent with our results. A relatively large yield for a 2-sec ^{123}Cd, as is indicated by the systematics to be discussed, would require relatively small ^{123}In and ^{123}In^m yields and a relatively large independent yield for ^{123}Sn^m, contrary to the systematics derived.

The yield values for 2.33-sec ^{125}In, 12.2-sec ^{125}In^m, and 9.64-d ^{125}Sn, and also for 1.12-sec ^{127}In, 3.7-sec ^{127}In^m, and 2.10-h ^{127}Sn were determined without consideration of silver or cadmium precursors. If ~0.5-sec cadmium precursors exist[28] and are formed in appreciable yield, the indium cumulative yields (Table III) would be lowered somewhat.

The yield value for 0.90-sec ^{128}In and 59.3-min ^{128}Sn were also determined without consideration of silver or cadmium precursors. The 6.5-sec ^{128}Sn^m, which decays to ^{128}Sn, and the individual isomeric states of ^{128}In, both of which have ~0.9-sec half-lives, could not be detected in our experiments. The standard-deviation errors given in Tables II–IV were propagated from errors determined in the least-squares analysis, the error in delay time (±0.4 sec), and the errors of yield values from the literature.

DISCUSSION

In order to interpret mass- and charge-distribution data for the A,Z region investigated, a new neutron-emission function, the average number of neutrons emitted, $\bar{\nu}_p$, to form products for each A, was derived. As described previously,[29,30] the function was derived from mass-yield data[26] by use of a modification of Terrell's method.[31] Parameters for the simple function were chosen to represent experimental data as well as possible; a comparison of the function with experimental data measured for fission fragments,[32–34] $\bar{\nu}_f$ vs A_f, and converted to values for products is shown in Fig. 5 ($A=A_f-\bar{\nu}_f$, $\bar{\nu}_p=\bar{\nu}_f$). The neutron-emission function decreases linearly from $\bar{\nu}_p=1.20$ at $A=121$ to $\bar{\nu}_p=0.54$ at $A=128$; in the complementary region ν_p increases approximately linearly from 1.86 at $A=103$ to 2.15 at $A=109$, reaching a maximum of 2.16 at $A=110$.

Figure 6 shows the mass-dispersion curve, i.e., independent yield, IN (%), vs average primary-fragment mass number, $A'=A+\bar{\nu}_p$, for complementary In and Tc isotopes. Indium yields plotted for $A=125-132$ are actually cumulative ones; they can be treated as independent yields, however, since the cumulative yields of cadmium precursors are estimated to be small. The cumulative yield of ^{123}In has been corrected for the cumulative yield of ^{123}Cd, as described later.

Indium yields from this investigation agree well with complementary technetium yields determined radiochemically,[9] which suggests that both yield sets are reliable and indicates that the derived neutron function is a reasonable one for the mass numbers considered. However, radiochemical yields for $A_{\rm In}>125$ and $A_{\rm Tc}<106$ are considerably lower than those determined mass spectrometrically[8] and those determined from recoil-separator measurements.[11,12]

It had been observed earlier[29] that small yields below about 0.1% are often too large from recoil-separator measurements, whereas larger yields agree well with radiochemical measurements. Also, small mass-spectrometric yields for Rb, Sr, Cs, and Ba fission products from thermal-neutron-induced fission of ^{235}U far from stability deviate from a Gaussian shape, and a "wing effect" was suggested by Schmid *et al.*[35] This wing effect was not observed for Rb and Cs yields from other mass-spectrometric measurements,[36] nor was it observed for krypton and xenon yields;[37,38] thus, it is possible that

TABLE IV. Fractional fission yields for thermal-neutron-induced fission of ^{235}U. The first yield is cumulative, the rest are independent for each A. Both isomers are included, where appropriate.

A	Ag	Cd	In	Sn
121	0.207±0.210	0.585±0.267	0.179±0.103	0.029±0.054
123			0.886±0.127	0.114±0.070
125			$0.559^{+0.179}_{-0.117}$	$0.441^{+0.169}_{-0.097}$
127			0.228±0.070	0.715±0.101
128			0.042±0.021	0.909±0.030

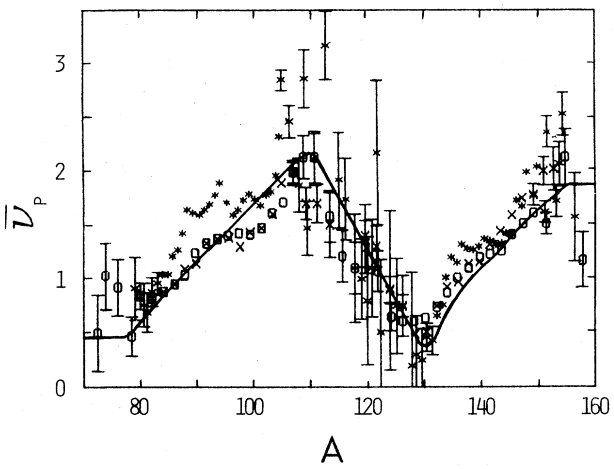

FIG. 5. Neutron emission function for thermal-neutron-induced fission of ^{235}U derived as described in the text. (——) derived function; (×,○,*) experimental data derived from plots in Refs. 32–34, respectively. Error bars are shown only for errors >0.1 in $\bar{\nu}_p$.

some small mass-spectrometric yields[8,35] may also be too large. Also, the mass-spectrometric In yields show an oscillation that is consistent with a sizable even-odd neutron effect, an effect not observed for other In,Tc yields plotted in Fig. 6.

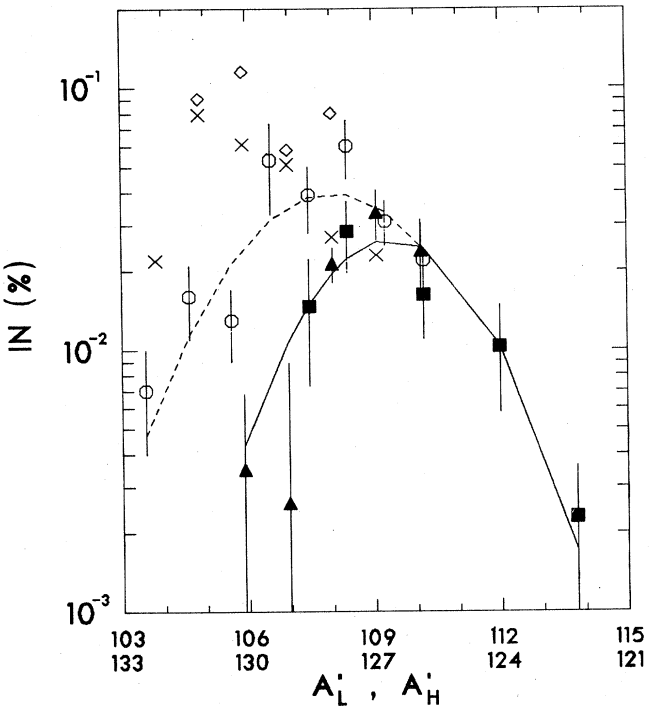

FIG. 6. Independent yields, IN, of In and Tc isotopes versus average fragment masses, A'_L and A'_H, for thermal-neutron-induced fission of ^{235}U. (■) In, radiochemical, this investigation; (▲) Tc, radiochemical, Ref. 9; (○) In, mass spectrometry, Ref. 8; (◇) Tc, Hiawatha separator, Ref. 11; (×) Tc, Lohengrin separator, Ref. 12; (——) Gaussian fit to (■) and (▲) points; and (— — —) Gaussian fit to (○) points.

Each method of measurement pushed to near its limit for small yields and/or short half-lives may have inherent systematic errors. Recoil-separator data could suffer from possible errors from fitting of Gaussian curves to low intensity tails of energy-loss spectra and from summation of incomplete data for various charge states and kinetic energies of fission products. For mass-spectrometric measurements major uncertainties include separation efficiency from the target, delay-time corrections, and impurities from isobars having much larger yields. The reliability of radiochemical determinations also could suffer from unexpected chemical behavior of newly formed fission products because of unusual oxidation states, complexes, etc., which could result from "hot-atom" or radiation-induced effects on fission products at very low concentrations. In addition, there is some uncertainty in the time of separation. It is difficult to prove the superiority of one type of measurement, so charge- and mass-distribution systematics deduced from different yield sets are discussed below.

The widths of mass-dispersion curves, $\sigma_{A'}$ (standard deviation), as well as the $\Delta A'$ function were calculated for radiochemically determined indium and technetium yields and for mass-spectrometrically determined indium yields by fitting the data with Gaussian mass-dispersion curves.[1,2] Even-odd effects were not considered. $\Delta A'$ is defined as follows:[1,2]

$$\Delta A' = \left[A'_p - Z\frac{A_F}{Z_F} \right]_H = \left[Z\frac{A_F}{Z_F} - A'_p \right]_L ,$$

where A'_p is the most probable average primary-fragment mass, Z is the atomic number, A is the mass number, F indicates a fissioning nucleus, and H and L refer to heavy and light fragments, respectively. Also, $\sigma_{A'}$ and $\Delta A'$ were calculated for other elements, as has been done before;[2,29] independent yields were obtained from Wahl's compilation.[39] The results are shown in Figs. 7 and 8.

The widths of mass-dispersion curves derived from the compiled yields and from radiochemically determined In,Tc and Sn,Mo yields increase slightly towards symmetry showing small deviations from an average value of about 1.5 u. Mass spectrometric data for $Z_H=49$ give a dispersion width of 2.3, an abrupt increase from the average. The $\Delta A'$ function shows a steady increase with decreasing Z_H peaking at $Z_H=50$. The sharp drop at $Z_H=49$ for $\Delta A'$ from radiochemical data is a reasonable approach to the expected $\Delta A'=0.0$ value for $Z_H=46$. The $\Delta A'$ from mass spectrometric yields does not show this sharp drop.

The elemental yield, $Y(Z=43,49)$, from radiochemical data is $0.11\pm0.01\,\%$, while the elemental yield from mass-spectrometric data is $0.22\pm0.03\,\%$; both values are much smaller than $Y(Z=42,50)=4.0\pm0.5\,\%$.

Widths, σ_Z, of charge-dispersion curves for the A's of interest were also studied. Charge dispersion describes the dependence of fractional-independent yields, FI, on Z for constant A. The procedure involved fitting Gaussian curves to FI data without even-odd effects.[1,2,29,30] The results are shown in Fig. 9. For $A=121$, point 1, all yields are reported in this paper. For $A=127$ and 128, points 4

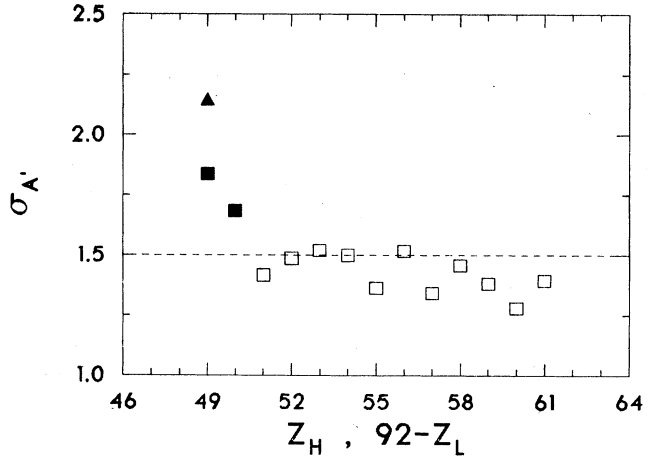

FIG. 7. Width of mass dispersion curves, $\sigma_{A'}$, as a function of atomic number Z for thermal-neutron-induced fission of ^{235}U. (■) radiochemical In,Sn yields, this investigation, radiochemical Tc yields, Ref. 9, and compiled Sn,Mo yields, Ref. 39; (▲) mass spectrometric In yields, Ref. 8; (□) compiled yields, Ref. 39; and (— — —) $\sigma_{A'}=1.5$, approximately average value from (■) and (□) points.

and 5, antimony yields were taken from Refs. 40 and 41, respectively. For $A=123$ and 125, points 2 and 3, only related values of yields exist, cumulative indium yields and independent tin yields, which are insufficient data to determine both Gaussian parameters, Z_p and σ_Z. Therefore, σ_Z for these mass numbers was assumed to be the average, 0.52, determined for other mass numbers[30] (the dashed line in Fig. 9). Yields for other A's were taken from Wahl's compilation[39] for similar calculations. The oscillation in σ_Z to the right of $Z_p=50$ is a result of the even-odd Z effect.[30]

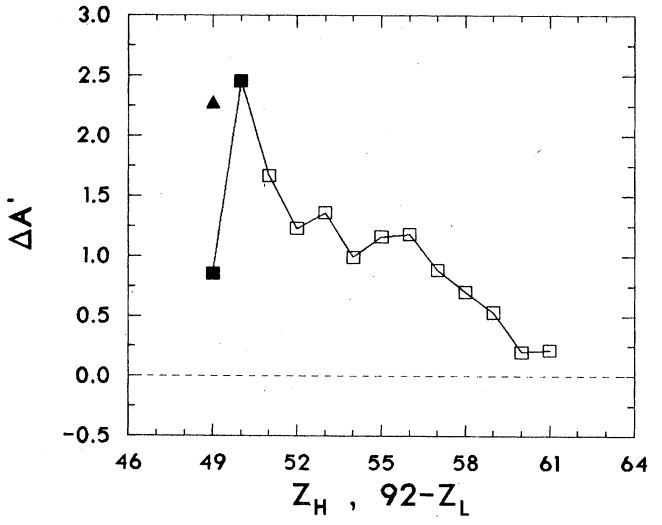

FIG. 8. $\Delta A'$ as a function of atomic number Z for thermal-neutron-induced fission of ^{235}U. (■) radiochemical In,Sn yields, this investigation, radiochemical Tc yields, Ref. 9, and compiled Sn,Mo yields, Ref. 39; (▲) mass spectrometric In yields, Ref. 8; (□) compiled yields, Ref. 39; and (— — —) $\Delta A'=0$.

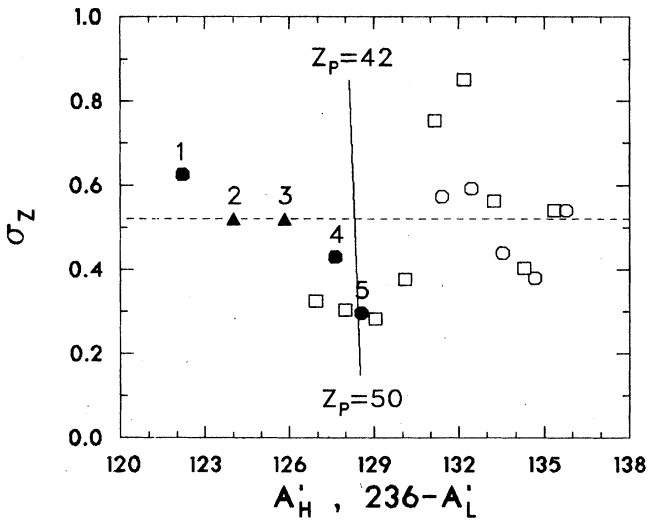

FIG. 9. Width of charge dispersion curves, σ_Z, as a function of average fragment mass for thermal-neutron-induced fission of ^{235}U. (●) heavy fragments, this investigation; (▲) points number 2,3 average σ_z assumed; (○) heavy fragments from compiled yields, Ref. 39; (□) light fragments from compiled yields, Ref. 39; nearly vertical line $Z_p=50,42$; and (— — —) $\sigma_Z=0.52$, average value, Ref. 30.

A plot of the ΔZ function is shown in Fig. 10. ΔZ is defined by

$$\Delta Z=[Z_p-Z(\mathrm{UCD})]_H=[Z(\mathrm{UCD})-Z_p]_L\ ,$$

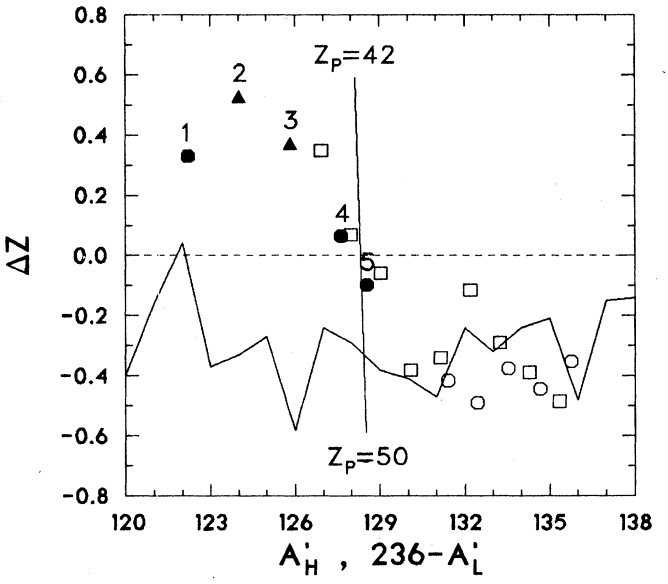

FIG. 10. ΔZ as a function of average fragment mass for thermal-neutron-induced fission of ^{235}U. (●) heavy fragments, this investigation; (▲) points number 2,3 average σ_Z assumed; (○) heavy fragments from compiled yields, Ref. 39; (□) light fragments from compiled yields, Ref. 39; (— — —) UCD line; nearly vertical line $Z_p=50,42$; and (——) scission point model, Ref. 6.

Z_p being the most probable charge for a charge dispersion curve, and $Z(\mathrm{UCD})=A'(Z_F/A_F)$, UCD indicating "unchanged charge distribution." To the right of $Z_p=50,42$ the ΔZ function has an average value of -0.45 and is modulated somewhat due to the even-odd Z effect. Near $Z=50$ the function undergoes an abrupt rise to $\Delta Z>0$. This structure has been noted previously,[12,29] but the observations were based on less data. The break near $Z=50$ was anticipated in Wolfsberg's compilation,[42] and the mass-spectrometrically determined indium yields are consistent with such a break.[8]

The details of structure for the ΔZ function near and below $Z_p=50$, in particular the range where $\Delta Z>0$, depend on the neutron function assumed and on the data sets used to derive the ΔZ function. The sharp break is well established, and it is probably associated with the effect of the fifty-proton shell on yields of fission-products with Z near 50.

If the peak of the neutron emission function was assumed to be near symmetry, the positive ΔZ values would be lowered, tending toward $\Delta Z=0$ at symmetry ($A'=118$) in a more obvious way than that shown in Fig. 10 (Ref. 1). The trends of both ΔZ and $\Delta A'$ (Fig. 8) to zero at symmetry ($Z=46$, $A'=118$) is expected since ^{236}U can fission symmetrically. This expectation has not been confirmed experimentally for low-energy fission reactions, but data for near symmetric fission of ^{233}U and ^{235}U induced by 40—100 MeV protons have been interpreted by the UCD postulate.[43]

The line in Fig. 10 shows the ΔZ function calculated by Wilkins *et al.* in their scission-point model.[6] Beyond the $Z_p=50$ region one finds semiquantitative agreement between model and data, but the model does not reproduce the structure near and below $Z_p=50$. A possible reason for this is that the model emphasizes the $N=82$ shell in this region, and the $Z=50$ shell is not energetically favored to occur together with the $N=82$ shell due to liquid-drop potential-energy considerations. The $Z=50$ shell may not be important in the heavy-mass peak region where the $N=82$ shell dominates according to Wilkins *et al.* However, on the light side of the heavy peak, where the transition from symmetric to asymmetric fission occurs, the fifty-proton shell appears to play an important role.

The cumulative yield of ^{123}Cd can be estimated to be $0.0037\pm0.0019\,\%$ from the assumed $\sigma_Z=0.52$, derived $\Delta Z=0.53$, and chain yield of $0.0158\pm0.0007\,\%$,[26] so the independent yield of ^{123}In, used earlier in the discussion, is $0.0103\pm0.0051\,\%$.

As indicated before, the Sn formation modes for 14-MeV-neutron-induced fission of ^{235}U are less useful than those for thermal-neutron-induced fission of ^{235}U, because no other data are available to supplement them. However, one can calculate from Table II that for $A=128$, where the effects of the $Z=50$ shell dominate, the ratio of the tin fraction formed independently to the fraction formed from indium decay is ~22 for thermal and ~7 for 14-MeV fission. Also, the independent yield of ^{128}In is ~20 times higher for 14-MeV fission than for thermal fission. Thus, the effect of the $Z=50$ shell on yields decreases at higher excitation energy.

CONCLUSIONS

The yields of indium and tin nuclides reported in this paper furnish additional evidence for the importance of the fifty-proton shell on the charge and mass distributions of fission products in the transition region ($A\approx120$—130) between symmetric and asymmetric fission. The fifty-proton effect on yields can be described in various ways. The ΔZ function from the Z_p model breaks sharply upward, from -0.45 to >0, when $Z_p\approx50$, i.e., Z_p remains close to 50 over several mass numbers. The $\Delta A'$ function for the A_p' model peaks at $Z=50$, and elemental yields fall sharply for Z's just under 50, i.e., from $Y(Z=50)=4.0\%$ to $Y(Z=49)=0.1\%$. At higher excitation energies the effect of the fifty-proton shell on yields decreases. Additional experiments will be required to resolve differences for small yields from radiochemical measurements and from physical ones and also to determine the behavior of the charge- and mass-distribution functions near symmetry.

ACKNOWLEDGMENTS

The authors wish to thank Dr. C. Gatrousis and Dr. R. A. Mayer for the loan of the SISAK system from the Lawrence Livermore Laboratory. Thanks are also due to the following people for their valuable contributions to our research: J. T. Hood and the Washington University cyclotron staff for providing irradiations; Prof. J. Rydberg and Dr. H. Reinhardt for advice concerning operation of the SISAK system and for prompt handling of orders and repairs; Dr. G. P. Ford for providing computer subroutines; T. N. Massey and Prof. R. P. Yaffe for instruction concerning the SISAK operation; H. K. Dworsky and D. Roman for assistance with computer programming; and L. Djordjevic for electronics assistance. Large portions of the work were extracted from the Ph.D. thesis of T. M. Semkow (Ref. 1). This work was supported in part by the National Science Foundation under Grants CHE-7602473 and CHE-8003325.

APPENDIX

As pointed out in the data reduction section, standard equations for radioactive decay and growth could not be applied to data from our experiments. In deriving the necessary equations, we used a matrix notation described by Ford *et al.*[44] However, explicit expressions for the decay-growth matrices, P and P^{-1}, were derived and are given below, rather than obtaining the matrices from diagonalization of a matrix A, as did Ford *et al.*

$$P_{j>i}=\begin{cases}\alpha, & j<i+2,\\ \alpha+\beta, & j=i+2,\\ \alpha+\beta+\gamma, & j>i+2,\end{cases}\qquad P_{ii}=1,\qquad P_{j<i}=0,$$

where

$$\alpha=\frac{A_{ji}}{\lambda_j-\lambda_i},\quad \beta=\sum_{k=i+1}^{j-1}\frac{A_{ki}A_{jk}}{(\lambda_k-\lambda_i)(\lambda_j-\lambda_i)},$$

$$\gamma=\sum_{m=2}^{j-i-1}\left[\sum_{x_1=i+1}^{j-m}\sum_{<x_2}^{j-m+1}\cdots\sum_{<x_m}^{j-1}\frac{A_{x_1 i}A_{jx_m}\prod_{k=2}^{m}A_{x_k x_{k-1}}}{(\lambda_j-\lambda_i)\prod_{k=1}^{m}(\lambda_{x_k}-\lambda_i)}\right],$$

where $A_{ji}=\lambda_i b_{ji}$ for $j>i$, $A_{ii}=-\lambda_i$, $A_{ji}=0$ for $j<i$, λ_i is a decay constant, and b_{ji} is a branching fraction of component i that decays to component j in a radioactive decay chain. P_{ji}^{-1} elements are similar to P_{ji} elements, except the indexes i and j are interchanged in the denominators.

To take care of the flow of solutions, we incorporated the tank-target model of Aronsson[15] in the decay-growth equations.[1] Solvent extraction models mentioned in the data reduction section were also included to describe the extraction in a closed circulating loop of solution.[1] The equation used for $A=121$ and 123 is given in the following:

$$\frac{I^{\text{org}}}{I^{\text{tot}}}=F+\frac{(1-F)P_n^{-1}CWP\left[f\,\text{diag}\left[e^{-\lambda_i\tau}\frac{1}{1+\lambda_i T}\right]+(1-f)\text{diag}\left[\frac{1-e^{-\lambda_i u}}{\lambda_i u}\right]\right]P^{-1}X}{\left[f\frac{1}{1+\lambda_n T}+(1-f)\right]P_n^{-1}X},$$

where I^{org} and I^{tot} are organic-phase and total intercept counting rates, respectively; $C=\text{diag}(c_i)$ is a matrix of the single-step extraction fractions, c_i;

$$W=\{\text{diag}(1)-P\,\text{diag}(e^{-\lambda_i u})P^{-1}[\text{diag}(1)-C]\}^{-1}$$

describes the extraction of precursors including looping; i is a component index for a radioactive decay chain; n indicates the last component, i.e., Sn; τ is the delay time; u is a looping time of the aqueous phase; T is a mean hold up time of the solution in the target; F is the total fraction of Sn extracted in a continuous system (this requires $c_n=0$ in the C matrix); f is a fraction of activity formed in the target; X is a vector of fractional independent yields, FI_i; and P_n^{-1} is the nth row of the P^{-1} matrix. diag denotes a diagonal matrix. For $A=125$, 127, and 128, since $T_{1/2}$ (precursors) $\ll u$, the following simplified equation was used:

$$\frac{I^{\text{org}}}{I^{\text{tot}}}=F+\frac{(1-F)fP_n^{-1}CP\,\text{diag}\left[e^{-\lambda_i\tau}\frac{1}{1+\lambda_i T}\right]P^{-1}X}{\left[f\frac{1}{1+\lambda_n T}+(1-f)\right]P_n^{-1}X}.$$

In order to have proper balance of FI_i yields to fractional cumulative yields of Sn, FC_n, corrected for decay effects, FI_i in X is replaced by $E_{ni}\text{FI}_i/P_{ni}^{-1}$. E_{ni} are elements of a row matrix E_n, which is similar to P_n^{-1}, but contains only branching ratios, not decay constants. Then

$$P_n^{-1}X=\sum_{i=1}^{n}P_{ni}^{-1}E_{ni}\text{FI}_i/P_{ni}^{-1}$$

$$=\sum_{i=1}^{n}E_{ni}\text{FI}_i=E_nX=\text{FC}_n\ .$$

The last yield branching equation was also used in calculations for the least-squares analysis. If none of the decays branch out of the chain this equation reduces the familiar $\sum\text{FI}_i=\text{FC}_n$. More details about the decay-growth calculation for a continuous irradiation-separation experiment, as well as a FORTRAN code to calculate the matrices, P, P^{-1}, and E, can be found in Ref. 1.

[1]T. M. Semkow, Ph.D. thesis, Washington University, St. Louis, 1983.

[2]A. C. Wahl, in *New Directions in Physics and Chemistry*, edited by N. R. Metropolis, and G.-C. Rota (Academic, New York, to be published).

[3]A. C. Wahl, in *Physics and Chemistry of Fission* (IAEA, Vienna, 1965), Vol. I, p. 317.

[4]D. Hoffman, in *Physics and Chemistry of Fission* (IAEA, Vienna, 1980), Vol. II, p. 275.

[5]J. F. Wild, E. K. Hulet, R. W. Lougheed, P. A. Baisden, J. H. Landrum, R. J. Dougan, and M. G. Mustafa, Phys. Rev. C **26**, 1531 (1982).

[6]B. D. Wilkins, E. P. Steinberg, and R. R. Chasman, Phys. Rev. C **14**, 1832 (1976).

[7]B. R. Erdal, A. C. Wahl, and R. L. Ferguson, J. Inorg. Nucl. Chem. **33**, 2763 (1971).

[8]M. Schmid and G. Engler, Z. Phys. A **311**, 113 (1983).

[9]T. Fassbender, Diplomarbeit, Universität Mainz, 1979.

[10]E. N. Vine and A. C. Wahl, J. Inorg. Nucl. Chem. **43**, 877 (1981).

[11]R. B. Strittmatter, Ph.D. thesis, University of Illinois, 1978.

[12]W. Lang, H.-G. Clerc, H. Wohlfarth, H. Schrader, and K.-H. Schmidt, Nucl. Phys. **A345**, 34 (1980).

[13]J. Rydberg, H. Persson, P. O. Aronsson, A. Selme, and G. Skarnemark, Hydrometallurgy **5**, 273 (1980).

[14]T. Semkow and A. C. Wahl, J. Radioanal. Chem. **79**, 93 (1983).

[15]P. O. Aronsson, Ph.D. thesis, Chalmers University of Technology, Göteborg, 1974.

[16]B. Fogelberg, L.-E. De Geer, K. Fransson, and M. Ugglas, Z. Phys. A **276**, 381 (1976).

[17]B. Grapengiesser, E. Lund, and G. Rudstam, J. Inorg. Nucl.

Chem. **36**, 2409 (1974).
[18]E. Lund, P. Hoff, K. Aleklett, D. Glomset, and G. Rudstam, Z. Phys. A **294**, 233 (1980).
[19]G. Engler and E. Ne'eman, Nucl. Phys. **A367**, 29 (1981).
[20]L.-E. De Geer and G. B. Holm, Phys. Rev. C **22**, 2163 (1980).
[21]B. Fogelberg and P. Carlé, Nucl. Phys. **A323**, 205 (1979).
[22]E. Lund and G. Rudstam, Phys. Rev. C **13**, 1544 (1976).
[23]B. R. Erdal and A. C. Wahl, J. Inorg. Nucl. Chem. **30**, 1985 (1968).
[24]J. B. Cumming, in United States Atomic Energy Commission Report No. NAS-NS-3107, 1962, p. 25.
[25]W. R. Busing and H. A. Levy, Oak Ridge National Laboratory Report No. ORNL-TM-271, 1962.
[26]B. F. Rider, Vallecitos Nuclear Center Report No. NEDO-12154-3(C), 1981.
[27]P. L. Reeder, R. A. Warner, and R. L. Gill, Phys. Rev. C **27**, 3002 (1983).
[28]P. L. Reeder, private communication.
[29]A. C. Wahl, in International Atomic Energy Agency Report No. INDC(NDS)-87, 1978, p. 215. (Contribution to review paper No. 11, Petten Meeting on Fission Product Nuclear Data, 1977.)
[30]A. C. Wahl, J. Radioanal. Chem. **55**, 111 (1980).
[31]J. Terrell, Phys. Rev. **127**, 880 (1962).
[32]J. W. Boldeman, A. R. de L. Musgrove, and R. L. Walsh, Aust. J. Phys. **24**, 821 (1971).
[33]E. E. Maslin, A. L. Rodgers, and W. G. F. Core, Phys. Rev. **164**, 1520 (1967).
[34]J. C. D. Milton and J. S. Fraser, in *Physics and Chemistry in Fission* (IAEA, Vienna, 1965), Vol. II, p. 39.
[35]M. Schmid, Y. Nir-El, G. Engler, and S. Amiel, J. Inorg. Nucl. Chem. **43**, 867 (1981).
[36]S. J. Balestrini, R. Decker, H. Wollnik, K. D. Wünsch, G. Jung, E. Koglin, and G. Siegert, Phys. Rev. C **20**, 2244 (1979).
[37]A. C. Wahl, J. Inorg. Nucl. Chem. **6**, 263 (1958).
[38]A. C. Wahl, R. L. Ferguson, D. R. Nethaway, D. E. Troutner, and K. Wolfsberg, Phys. Rev. **126**, 1112 (1962).
[39]A. C. Wahl (unpublished).
[40]D. E. Troutner, A. C. Wahl, and R. L. Ferguson, Phys. Rev. **134**, B1027 (1964).
[41]M. M. Fowler and A. C. Wahl, J. Inorg. Nucl. Chem. **36**, 1201 (1974).
[42]K. Wolfsberg, Los Alamos National Laboratory Report No. LA-5553MS, 1974.
[43]P. A. Beeley, L. Yaffe, M. Chatterjee, H. Dautet, and J. K. P. Lee, Phys. Rev. C **28**, 1188 (1983).
[44]G. P. Ford, K. Wolfsberg, and B. R. Erdal, Phys. Rev. C **30**, 195 (1984).